Electronic Supplementary Material (ESI) for Sensors & Diagnostics.

Supporting Information

A fluorescent sp^2c-covalent organic polymer with aggregation-induced emission unit to suppress aggregation-induced quenching for sensing furazolidone

Xinyi Wang, Lijuan Kuang, Meiling Ye, Liangmei Zou, Li Wang* and Yonghai Song*

College of Chemistry and Chemical Engineering, Jiangxi Normal University, 99 Ziyang Avenue, Nanchang 330022, China.

Materials

Benzo[1,2-b:3,4-b':5,6-b"]trithiophene-2,5,8-tricarbaldehyde, p-xylylene dicyanide (98.0%, BTT) and benzaldehyde (99.0%) were bought from the Jilin Chinese Academy of Sciences - Yanshen Technology Co., Ltd. (Changchun, China). Furazolidone (98.0%, FZD) and ascorbic acid (99.0%) and other reagents used in interference experiments were purchased from Shanghai Aladdin Chemical Co., Ltd. (Shanghai, China). Sodium chloride (99.0%), potassium chloride (99.0%) and other reagents were purchased from Beijing Yinokai Technology Co., Ltd. (Beijing, China). All reagents were analytical grade and could be used without further purification. All solutions were prepared with ultrapure water and purified by millipore-Q system (18.2 MΩ cm^{-1}).

Instruments

All excitation and emission spectra were measured on a Hitachi F-7000 fluorescence spectrophotometer at a scanning speed of 1200 nm min^{-1}. Uv-vis absorption spectra were recorded by UV-vis spectrometer (Hitachi U-3900H). Fourier Transform infrared spectroscopy (FTIR) was measured by a Perkin-Elmer 200 spectrometer using potassium bromide tablet method with a wavelength range of 400 ~ 4000 cm^{-1}. The scanning electron microscope (SEM) images were determined by Hitachi S3400N SEM. Atomic force microscopy (AFM) image was collected by Bruker Nano-scope V (MultiMode 8) with ScanAsyst mode under atmosphere.. X-ray diffraction (XRD) data were collected with Cu K Kα radiation (λ=1.54056 A, 40 kV, 200 mA) on A D/Max 2500 V/PC X-ray powder diffractometer. N_2 adsorption and desorption isothermal test was carried out by Autosorb-iQ (Quantachrome) under a liquid nitrogen atmosphere of 77 K.

Optimize conditions of probe dosage and pH of the solution

In order to test the sensing performance of $COP_{PDAN\text{-}BTT}$ and $COP_{PDAN\text{-}TF}$ for FZD and obtain better detection results, the amount of probe and the pH of the detection environment were optimized. Firstly, the probe dosage was optimized. The fluorescence intensity of $COP_{PDAN\text{-}BTT}$ increased gradually with the increase of $COP_{PDAN\text{-}BTT}$ concentration, and reached the maximum value when the concentration reached 120 μg mL^{-1} (Fig. S4a). After that, the fluorescence intensity of $COP_{PDAN\text{-}BTT}$ was basically unchanged, and the solution still showed obvious Dundahl effect. Therefore, 120 μg mL^{-1} was selected as the optimal probe concentration of $COP_{PDAN\text{-}BTT}$. As shown in Fig. S4b, with the increase of concentration, the fluorescence intensity of $COP_{PDAN\text{-}TF}$ at 430 nm continuously increased without any trend of decrease, which reflects the AIE property of $COP_{PDAN\text{-}TF}$. Because $COP_{PDAN\text{-}TF}$ has higher fluorescence intensity at 120 μg mL^{-1}, 120 μg mL^{-1} was selected as the probe concentration of $COP_{PDAN\text{-}TF}$ for subsequent detection. Next, the pH of the solution is optimized. As shown in Fig. S4c and d, the fluorescence of $COP_{PDAN\text{-}BTT}$ remains stable under neutral and alkaline conditions, but the fluorescence intensity decreases under acidic conditions, while $COP_{PDAN\text{-}TF}$ remains stable under acidic, neutral and alkaline conditions. The decrease of fluorescence intensity of $COP_{PDAN\text{-}BTT}$ under acidic conditions can be attributed to the fact that BTT is easy to be protonated under acidic conditions. The greater the acidity of the solution, the more severe protonation of $COP_{PDAN\text{-}BTT}$ and the lower the fluorescence intensity. Since $COP_{PDAN\text{-}BTT}$ remained stable in the range of pH=7~10, subsequent detection was performed at pH=8. However, $COP_{PDAN\text{-}TF}$ has high stability under acidic, neutral and alkaline conditions, so the most commonly used PBS with pH=7 was selected as the test environment. Then, the optical stability was tested under optimized conditions. As shown in Fig. S5, the fluorescence intensity of $COP_{PDAN\text{-}BTT}$ and $COP_{PDAN\text{-}TF}$ both maintained high stability within 600s.

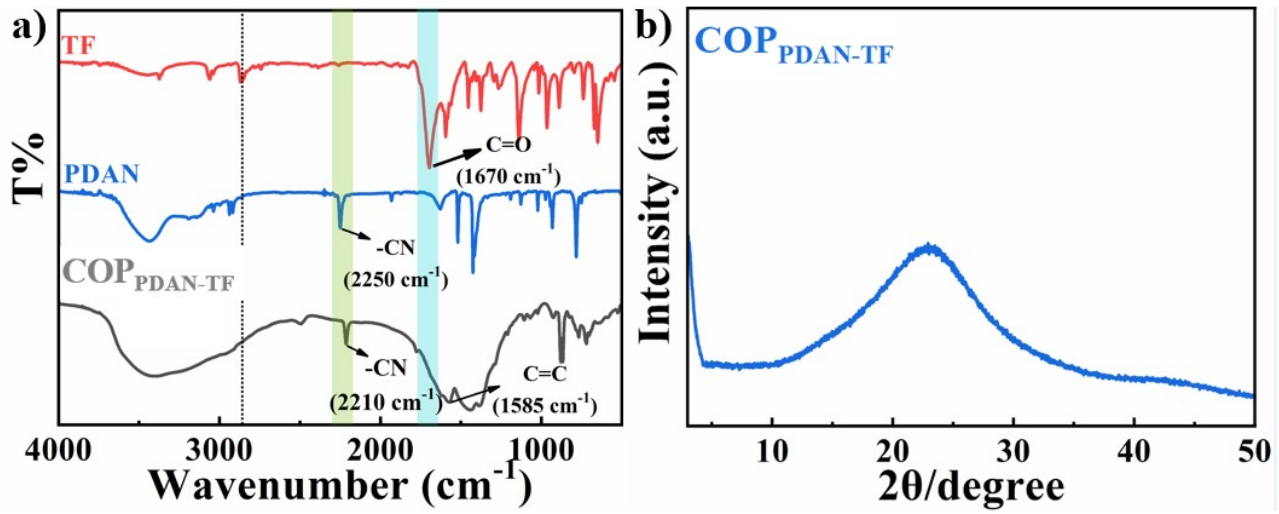

Fig. S1. (a)FTIR spectra of $COP_{PDAN-TF}$ and their monomers; (b)XRD patterns of $COP_{PDAN-TF}$.

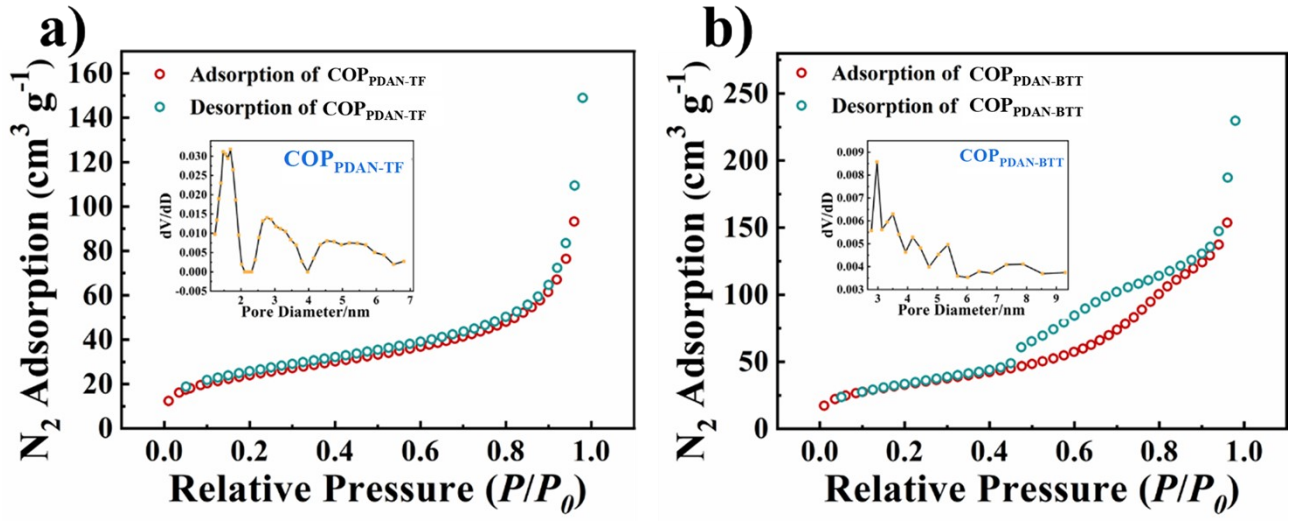

Fig. S2. N_2 adsorption/desorption isotherms and pore size distributions of $COP_{PDAN-TF}$ (a), $COP_{PDAN-BTT}$ (b).

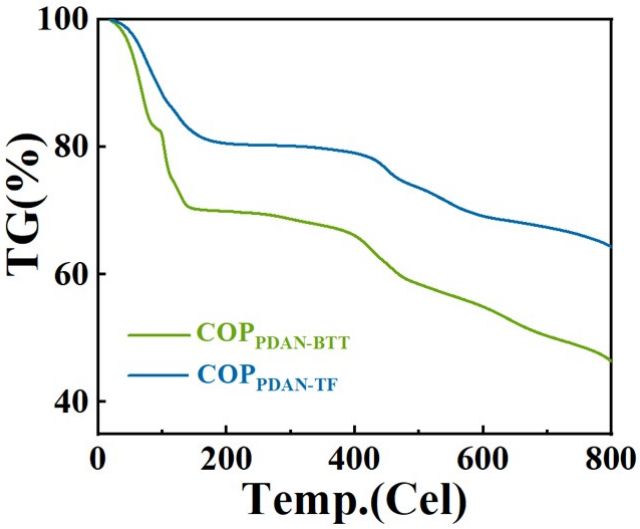

Fig. S3: Thermogravimetric analyses of $COP_{PDAN\text{-}BTT}$ and $COP_{PDAN\text{-}TF}$ under N_2 atmosphere.

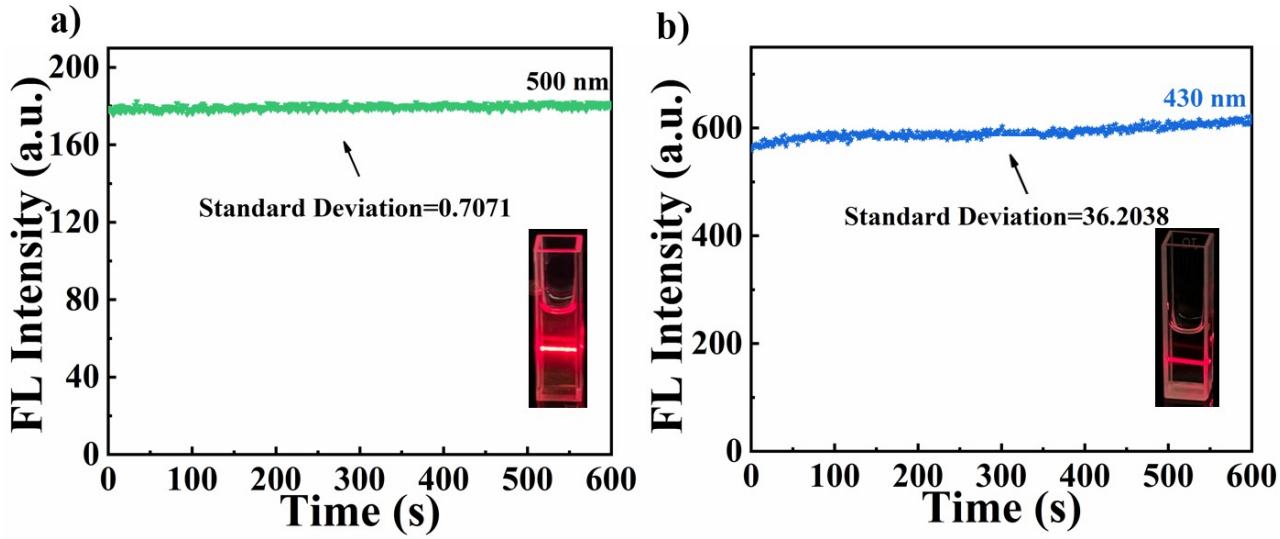

Fig. S4. (a) Changes in fluorescence intensity of $COP_{PDAN\text{-}BTT}$ and (b) $COP_{PDAN\text{-}TF}$ over 600 s consecutively

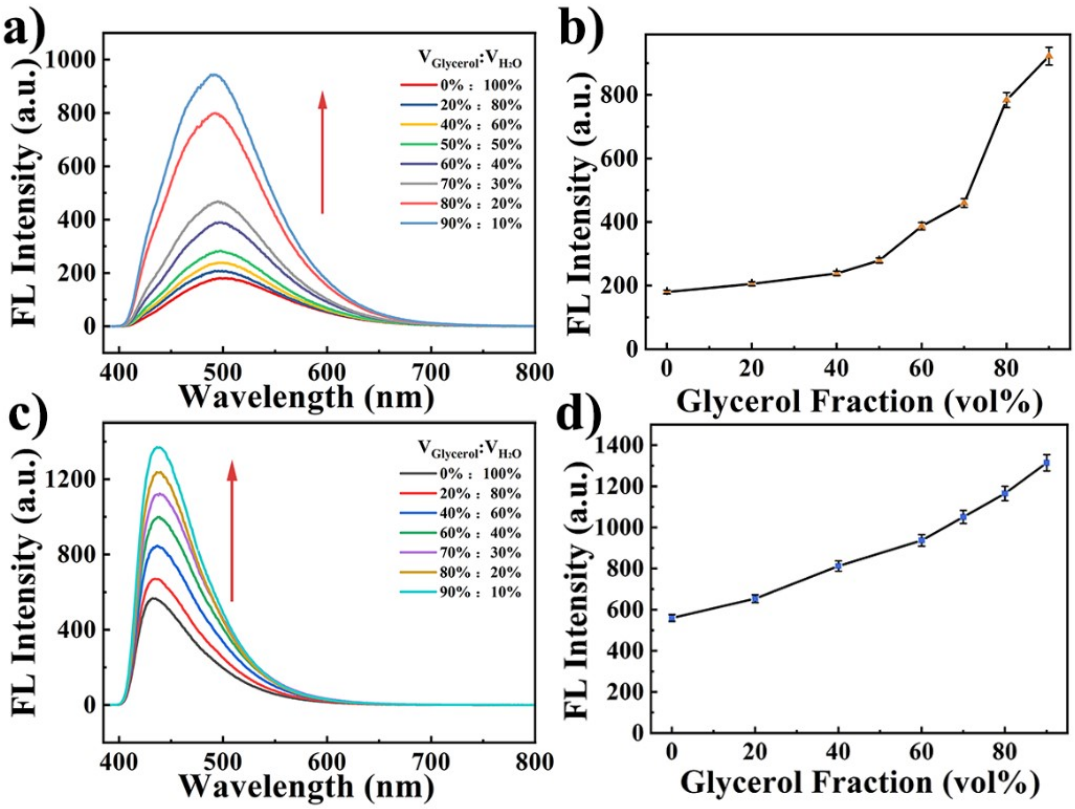

Fig. S5. (a) fluorescence emission spectra and (b) fluorescence intensity fold plots of $COP_{PDAN\text{-}BTT}$ in different propanol:water ratios; (c) fluorescence emission spectra and (d) fluorescence intensity fold plots of $COP_{PDAN\text{-}TF}$ in different propanol:water ratios.

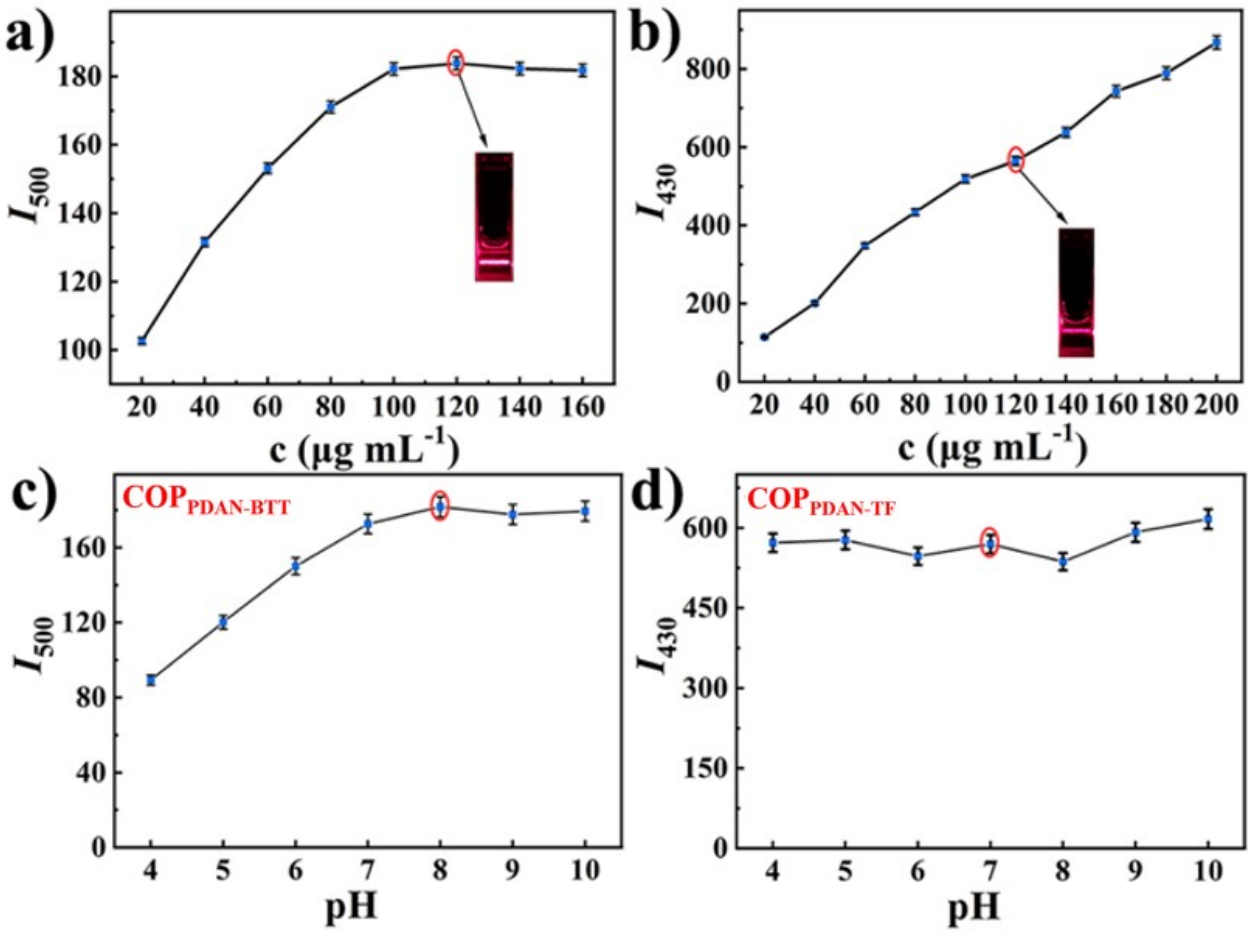

Fig. S6. (a) Folding line graph of fluorescence emission intensity of $COP_{PDAN-BTT}$ solution at different concentrations (inset: Tindal effect of $COP_{PDAN-BTT}$); (b) Folding line graph of fluorescence emission intensity of $COP_{PDAN-TF}$ solution at different concentrations (inset: Tindal effect of $COP_{PDAN-TF}$); (c) Folding line graph of fluorescence emission intensity of $COP_{PDAN-BTT}$ at different pH values; (d) Folding line graph of fluorescence emission intensity of $COP_{PDAN-TF}$ at different pH values.

Table S1. Different fluorescence probe for FZD detection.

Detection method	Probes	Detection limit	Ref.
Electrochemical method	COF@NH_2-CNT/GCE[a]	0.0775 μM	1
Raman spectroscopy	Ag NW-paper hydrophilichydrophobic substrate[b]	10 μg mL^{-1}	2
fluorescence method	ZnMOF	0.69 μM	3
fluorescence method	F-CTF-1	13.35 ppb	4
fluorescence method	Dy-TCPB[c]	0.0482 μM	5
fluorescence method	Al-MOF	0.583 μM	6
fluorescence method	$COP_{PDAN-BTT}$	0.011 μg mL^{-1} （0.049μM）	This work
fluorescence method	$COP_{PDAN-TF}$	0.023 μg mL^{-1} （0.101 μM）	This work

a：NH_2-CNT=amino-functionalized carbon nanotube；GCE=glassy carbon electrode

b：Ag NWs=Ag nanowires

c：H_3TCPB=1,3,5-tris(1-(2-carboxyphenyl)-1H-pyrazol-3-yl) benzene

Table S2. The recovery test of FZD was performed on the actual samples.

Probes	Actual samples	Addition value （μg mL^{-1}）	Detection value （μg mL^{-1}）	Recovery (%)
$COP_{PDAN-BTT}$	Lake water	0	Not detected	------
		5	4.79	95.8%
		10	9.93	99.3%
		20	20.36	101.8%
$COP_{PDAN-TF}$	Lake water	0	Not detected	------
		5	5.12	102.4%
		10	10.26	102.6%
		20	19.85	99.2%

References

1. Y. Sun, G. I. N. Waterhouse, L. Xu, X. Qiao and Z. Xu, *Sensors and Actuators B: Chemical*, 2020, **321**, 128501.
2. H. Sun, X. Li, Z. Hu, C. Gu, D. Chen, J. Wang, B. Li, T. Jiang and X. Zhou, *Applied Surface Science*, 2021, **556**, 149748.
3. Z. Cong, Z. Song, Y. Ma, M. Zhu, Y. Zhang, S. Wu and E. Gao, *Chemistry – An Asian Journal*, 2021, **16**, 1773-1779.
4. Y. Tang, H. Huang, W. Xue, Y. Chang, Y. Li, X. Guo and C. Zhong, *Chemical Engineering Journal*, 2020, **384**, 123382.
5. S. Wu, M. Zhu, Y. Zhang, M. Kosinova, V. P. Fedin and E. Gao, *Chemistry*, 2020, **26**, 3137-3144.
6. X. Yue, Z. Zhou, M. Li, M. Jie, B. Xu and Y. Bai, *Food Chemistry*, 2022, **367**, 130763.